AUT Journal of Electrical Engineering
10.22060/EEJ.2026.25827.6010

Robust ANN-Assisted Laguerre-EDW MPC for LFC of Renewable-Integrated Microgrids

Ritanjali Behera

Department of Electrical Engineering, Parala Maharaja Engineering College, Berhampur, Odisha, India
Email: beheraritanjali67@gmail.com

Abstract

This paper proposes an optimal tuning framework based on artificial neural networks for Laguerre function-based model predictive control using exponential data weighting (ANN-Laguerre-EDW MPC) applied to load frequency control (LFC) in renewable-integrated microgrids. The proposed approach eliminates the need for iterative optimization strategies by utilizing an ANN as a surrogate model to learn the relationship between controller settings and system performance. The approach is evaluated against conventional PID, MPC, Laguerre-EDW MPC, and PSO-based Laguerre-EDW MPC approaches under both step and random load perturbation conditions. Simulation results indicate that the proposed approach achieves up to a 68% reduction in the performance index (ISE) value relative to the other approaches, while facilitating smoother control actions and minimizing frequency oscillations. Moreover, the approach significantly decreases computing time by as much as 95% relative to PSO-based optimization, underscoring its computational efficiency and suitability for practical microgrid control implementation. The proposed LFC approach is further substantiated through sensitivity analysis against parametric uncertainty and statistical analysis, affirming its robustness and reliable performance.

Keywords: artificial neural networks, load frequency control, microgrids, model predictive control, optimization

1 Introduction

LFC is a critical element of modern power system operation, responsible for sustaining system frequency within acceptable bounds despite ongoing load fluctuations and disruptions. The growing incorporation of renewable energy sources, such as wind and solar, has significantly increased the complexity of frequency control in microgrids due to the stochastic and intermittent characteristics of generation [1], [2], [3]. These fluctuations create uncertainties that undermine system stability and complicate conventional control methods. Furthermore, the diminished system inertia in renewable-dominated microgrids worsens frequency fluctuations, necessitating rapid and precise control solutions for dependable operation.

Conventional control strategies, such as PID controllers, are extensively utilized owing to their straightforwardness and ease of implementation. Nevertheless, PID controllers demonstrate constrained robustness and inadequate flexibility in highly dynamic and nonlinear operating situations characteristic of renewable-integrated power systems [4], [5]. Their fixed-parameter characteristics render them inadequate for managing quick variations and uncertainty in microgrid settings. To address these limitations, sophisticated control systems such as MPC have garnered significant interest. MPC enables the explicit management of system limitations and forecasting of future system behavior, thereby enhancing dynamic performance and robustness

AUT Journal of Electrical Engineering
10.22060/EEJ.2026.25827.6010

Nomenclature

Symbol	Description
T	Time index
$\Delta f(t)$	Frequency deviation
$\Delta P_{pv}(t)$	Photovoltaic power deviation
$\Delta P_{wtg}(t)$	Wind turbine generator power deviation
$P_{load}(t)$	Load demand
$P_{besu}(t)$	Battery energy storage unit power
$P_{fesu}(t)$	Flywheel energy storage unit power
ΔP_g	Governor output power deviation
ΔP_{fc}	Fuel cell power deviation
ΔP_m	Mechanical power deviation
ΔP_L	Load disturbance
H	Inertia constant
D	Damping coefficient
R	Speed regulation parameter
T_g	Governor time constant
T_t	Turbine time constant
T_{pv}	PV system time constant
T_{wtg}	Wind turbine time constant
$x(t)$	State vector
$u(t)$	Control input vector
$d(t)$	Disturbance vector
A, B, E	System matrices
A_d, B_d, E_d	Discrete-time system matrices
T_s	Sampling time
J_{MPC}	Quadratic cost function
N_p	Prediction horizon
N_c	Control horizon
Q, R	Weighting matrices
$\eta_j(k)$	Laguerre coefficients
$l_j(i)$	Laguerre basis functions
A	Laguerre pole parameter
Λ	Exponential weighting factor
$\hat{J}$	Predicted cost from ANN
Θ	ANN parameters
ISE	Integral Square Error

10.22060/EEJ.2026.25827.6010

[2], [6]. MPC offers a structured framework for multi-variable control issues, especially advantageous in interconnected and hybrid energy systems.

In spite of its benefits, conventional MPC is restricted by significant processing demands arising from online optimization, hence constraining its real-time application. To resolve this issue, Laguerre function-based MPC has been introduced to diminish the complexity of the control problem by parameterizing the control trajectory [7]. Moreover, the integration of EDW improves transient response by prioritizing current system dynamics. These modifications considerably enhance computational efficiency while preserving acceptable control performance. The efficacy of Laguerre-EDW MPC is acutely sensitive to the choice of critical parameters, including the Laguerre pole and weighting factor, rendering the tuning procedure complex and contingent upon specific problems.

Recently, metaheuristic optimization techniques including PSO, have been extensively utilized for controller tuning in LFC issues [8]. The tuning of MPC using PSO enhances performance relative to traditional approaches by exploring near-optimal parameter configurations inside intricate solution spaces. Nevertheless, these methods frequently necessitate several simulations and repetitive calculations, leading to increased computational burden. This restricts their applicability in real-time or adaptive control situations, particularly in extensive or rapidly changing systems.

Artificial intelligence (AI) methodologies, especially ANN, exhibit significant promise in control optimization owing to their capacity to approximate intricate nonlinear mappings and diminish online computational demands [9], [10]. Recent studies have also explored high-fidelity data-driven equivalence models for renewable-integrated multi-microgrids using NARX neural networks [11]. Hybrid approaches integrating ANNs with MPC have exhibited enhanced efficacy in power system regulation applications [12]. Table 1 encapsulates recent AI/ANN-assisted approaches for LFC and MPC-based power system applications and underscores the research gap addressed by the proposed approach. ANN-based models serve as effective surrogate models, facilitating swift estimation of optimal control parameters without necessitating recurrent tuning. The use of ANN as a surrogate optimization instrument for calibrating Laguerre-based MPC parameters in microgrid LFC remains mostly unexplored.

Taking inspiration from these facts, this research provides an ANN-based optimal tuning framework for Laguerre-EDW MPC for LFC of renewable-integrated microgrids. The proposed approach involves training the ANN to understand the correlation between controller parameters and system performance, facilitating swift and effective parameter optimization. This greatly decreases computing demands while maintaining superior control performance. The proposed approach is evaluated against conventional PID, conventional MPC, Laguerre-EDW MPC, and PSO-tuned MPC controllers to illustrate its efficacy across various operating scenarios.

1.1 Research gap and novelty

Despite significant advancements in MPC-based LFC, some problems persist. The Laguerre-EDW MPC formulation mitigates the online computing demands of conventional MPC; however, its efficacy is significantly influenced by the appropriate selection of the Laguerre pole and the exponential weighting factor. These parameters collectively affect prediction accuracy, transient response, damping characteristics, and control effort, leading to a nonlinear coupled tuning issue for which no systematic analytical design methodology exists. As a result, controller tuning is typically executed via repeated simulations or iterative metaheuristic optimization, resulting in heightened processing demands.

Although ANN-based surrogate optimization has been successfully applied in various engineering domains, its application to the computationally efficient tuning of Laguerre-EDW MPC parameters for renewable-integrated microgrid LFC has received limited attention. Motivated by this research gap, this study utilizes an offline-trained ANN as a surrogate

Table 1: Comparison of recent AI/ANN-assisted approaches for LFC and MPC-based power system applications.

Reference	AI Technique	Controller	Role of AI	Main Limitation	Research Gap Addressed
Sengar et al. [13]	Hybrid Neural Network (LF-HNN)	Predictive LFC	Neural network predicts system behaviour for frequency regulation.	Does not employ MPC or surrogate optimization for controller parameter tuning.	Motivates the use of ANN as a surrogate optimization model for efficient Laguerre-EDW MPC parameter tuning rather than as a predictive controller.
Saadatmand et al. [14]	Deep Neural Network (DNN)	Model-Free Predictive Controller	DNN learns system dynamics to enable model-free predictive control.	Improves power and frequency regulation without requiring an explicit system model.	Does not address offline surrogate tuning of MPC parameters for renewable-integrated microgrids.
Hassan et al. [15]	Sooty Terns Optimization	MPC	Metaheuristic optimization is employed to determine MPC parameters.	Requires repeated iterative optimization with high computational cost.	Motivates replacing computationally intensive iterative optimization with a trained ANN surrogate model.
AlMajidi et al. [16]	PSO-Optimized ANN	ANN Controller	ANN directly performs frequency regulation following PSO-based tuning.	ANN replaces the controller and does not preserve the MPC structure.	Preserves the original Laguerre-EDW MPC while utilizing ANN only for rapid parameter estimation.
Dashtar et al. [17]	Hybrid GA–ANN	Microgrid Controller	Genetic algorithm optimizes ANN for generation scheduling and transient	No Laguerre-based MPC formulation or surrogate optimization mechanism is	Extends ANN application to computationally efficient surrogate tuning of Laguerre-EDW MPC

10.22060/EEJ.2026.25827.6010

			improvement.	presented.	parameters for microgrid LFC.
Yaghoubi et al. [18]	Constrained Neural MPC	MPC	Neural network predicts future plant behaviour within the MPC framework.	Primarily reviews MPC developments and does not present ANN-assisted surrogate optimization for controller tuning.	Motivates the development of ANN-based surrogate optimization to reduce computational complexity while preserving the MPC framework.
Ma et al. [19]	Agent-Based AI	Energy Management	AI coordinates distributed energy resources for resilient and optimal scheduling.	Focuses on energy management rather than load frequency control.	Highlights the need for computationally efficient ANN-assisted MPC tuning dedicated to secondary frequency regulation.
Tran et al. [20]	Learning-Based Sliding Mode	Sliding Mode Controller	Learning mechanism improves robustness against system disturbances.	Not based on MPC and does not perform ANN-assisted parameter optimization.	Combines the advantages of MPC and ANN-based surrogate optimization to achieve computationally efficient controller tuning.
Shehu et al. [21]	Hierarchical AI-Based Energy Management	Hierarchical Control	AI-enabled hierarchical control and energy management for standalone microgrids.	Focuses on supervisory control and energy management rather than MPC parameter tuning.	Motivates the development of an ANN-assisted surrogate optimization framework specifically for Laguerre-EDW MPC-based load frequency control.
Proposed Work	**Offline-Trained ANN**	**Laguerre-EDW MPC**	**ANN functions as a surrogate optimization model to estimate the optimal Laguerre pole and exponential weighting factor after offline training.**	**Requires offline dataset generation; online adaptive learning is not considered.**	**Addresses the computational limitations of iterative MPC tuning by enabling rapid parameter estimation while preserving the original Laguerre-EDW MPC formulation, thereby achieving improved frequency regulation in renewable-**

integrated microgrids.

optimization model to swiftly forecast near-optimal controller parameters, thus obviating the need for repetitive iterative optimization while preserving acceptable control performance.

Based on the above discussion, the main contributions of this work are summarized as follows:

- A framework utilizing an ANN-assisted surrogate optimization is established for the computationally efficient tuning of the Laguerre pole and exponential weighting factor in Laguerre-EDW MPC for renewable-integrated microgrid LFC, thereby eliminating the need for repetitive iterative optimization following offline training.
- The proposed framework is thoroughly tested against deterministic and stochastic load disturbances by dynamic, statistical, sensitivity, and computational analyses, showcasing enhanced frequency regulation at a substantially reduced computing cost compared to PSO-based tuning.

The subsequent sections of this paper are structured as follows. Section 2 presents the microgrid system modeling. Section 3 explores the Laguerre-EDW MPC formulation. Section 4 discusses the proposed optimization framework based on ANN. Section 5 outlines the simulation outcomes and subsequent discussions. Ultimately, Section 6 concludes the paper along with providing possible future scopes.

2 System Modeling of the Microgrid

This section establishes the dynamic modeling of the renewable-integrated microgrid utilized for LFC. The adopted model relies on the prevalent microgrid framework detailed in [13], which has been extensively employed in LFC research owing to its capacity to encapsulate the dynamics of distributed generation and energy storage systems. Microgrid modeling and control have been extensively examined in the literature [11], [14], [15], ranging from simplified transfer-function models for controller design to high-fidelity data-driven equivalence models for renewable-dominated multi-microgrids.

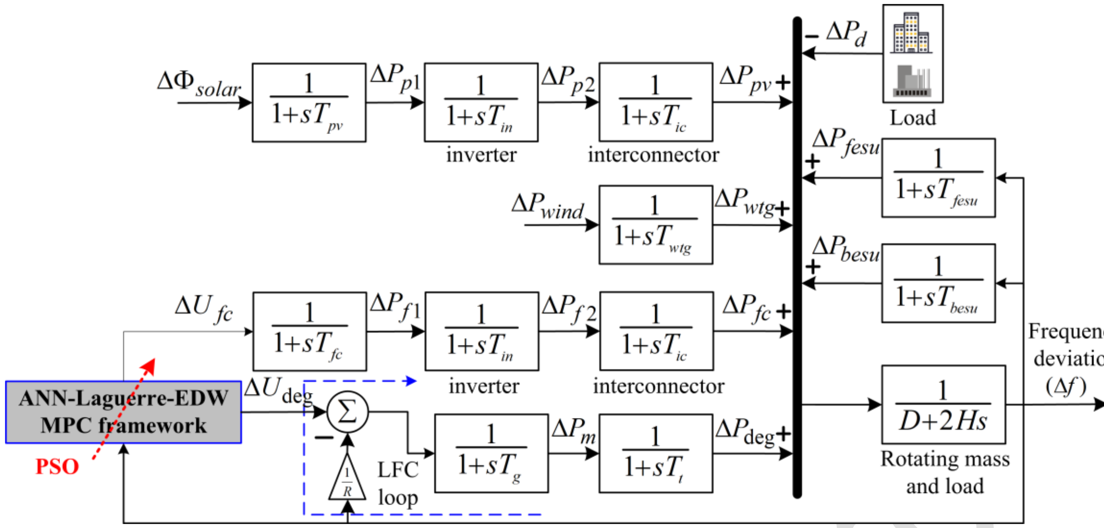

Figure 1: Model of microgrid used for the proposed ANN-Laguerre-EDW MPC LFC framework

2.1 Microgrid Configuration

The examined microgrid (shown in Fig. 1) comprises a diesel engine generator (DEG), fuel cell (FC), photovoltaic (PV) system, wind turbine generator (WTG), battery energy storage unit (BESU), and flywheel energy storage unit (FESU). The components are interconnected through power electronic interfaces and synchronized to uphold system frequency stability. Hybrid configurations have been extensively utilized in contemporary microgrid layouts to improve dependability and flexibility [3], [16]. The entire system experiences load disruptions and variations in renewable power, which substantially affect frequency dynamics. PV and WTG units are excluded from the LFC loop due to their non-dispatchable nature and their output is contingent upon environmental factors rather than control inputs. Consequently, they function as power disturbances rather than controllable entities for frequency regulation. Conversely, DEG and FC are dispatchable and controlled sources, rendering them appropriate for involvement in the LFC loop [17], [18].

This work employs first-order transfer function models to represent the various microgrid subsystems as shown in Fig. 1. These streamlined dynamic models are deliberately utilized to encapsulate the prevailing low-frequency dynamics that dictate LFC, while preserving a manageable framework for controller development and performance assessment. Reduced-order representations are extensively utilized in LFC research, as frequency control is predominantly influenced by the collective electromechanical response rather than intricate converter switching dynamics or electromagnetic transients. While high-fidelity nonlinear and data-driven models offer more detailed representations of renewable energy systems, they substantially elevate computational complexity and exceed the parameters of the current controller-focused study.

2.2 Dynamic Modeling of System Components

The system frequency dynamics are governed by the swing equation, representing the net power imbalance in the microgrid. Accordingly, the frequency deviation is expressed by (1)

10.22060/EEJ.2026.25827.6010

$$\Delta\dot{f}(t) = \frac{1}{2H}\left(\Delta P_{deg} + \Delta P_{fc} + \Delta P_{besu} + \Delta P_{fesu} + \Delta P_{pv} + \Delta P_{wtg} - \Delta P_d - D\Delta f\right) \quad (1)$$

where Δf denotes the frequency deviation, H is the inertia constant, and D is the damping coefficient. The terms ΔP_{pv} and ΔP_{wtg} represent renewable power variations, which are treated as disturbances due to their intermittent and non-dispatchable nature, while ΔP_{deg}, ΔP_{fc}, ΔP_{besu}, and ΔP_{fesu} correspond to the generation units participating in LFC.

The DEG is modeled using a standard governor-turbine system widely adopted in LFC studies given by (2)-(3) [19]

$$\Delta\dot{P}_m = \frac{1}{T_g}\left(-\Delta P_m - \frac{1}{R}\Delta f + \Delta U_{deg}\right) \quad (2)$$

$$\Delta\dot{P}_{deg} = \frac{1}{T_t}\left(-\Delta P_{deg} + \Delta P_m\right) \quad (3)$$

where ΔP_m and ΔP_{deg} denote the governor and mechanical power outputs, respectively, T_g and T_t are the governor and turbine time constants, R is the speed regulation parameter, and ΔU_{deg} is the control input obtained from the proposed controller.

The FC is modeled as a first-order dynamic system due to its relatively slower electrochemical response characteristics given by (4)-(6) [13]

$$\Delta\dot{P}_{fc}(t) = \frac{1}{T_{ic}}\left(-\Delta P_{fc} + \Delta P_{f2}\right) \quad (4)$$

$$\Delta\dot{P}_{f2}(t) = \frac{1}{T_{in}}\left(-\Delta P_{f2} + \Delta P_{f1}\right) \quad (5)$$

$$\Delta\dot{P}_{f1}(t) = \frac{1}{T_{fc}}\left(-\Delta P_{f1} + \Delta U_{fc}\right) \quad (6)$$

where ΔP_{fc} represents the fuel cell output power, T_{fc} is the fuel cell time constant, and ΔU_{fc} is the control input. The output power is subsequently processed through inverter and interconnection dynamics before being injected into the microgrid.

Renewable energy sources such as PV and WTG units are modeled using first-order transfer functions to capture their dynamic response to variations in environmental conditions expressed by (7)-(10) [14]

$$\Delta\dot{P}_{pv}(t) = \frac{1}{T_{ic}}\left(-\Delta P_{pv} + \Delta P_{p2}\right) \quad (7)$$

$$\Delta\dot{P}_{p2}(t) = \frac{1}{T_{in}}\left(-\Delta P_{p2} + \Delta P_{p1}\right) \quad (8)$$

$$\Delta\dot{P}_{p1}(t) = \frac{1}{T_{pv}}\left(-\Delta P_{p1} + \Delta\phi_{solar}\right) \quad (9)$$

$$\Delta\dot{P}_{wtg} = \frac{1}{T_{wtg}}\left(-\Delta P_{wtg} + \Delta P_{wind}\right) \quad (10)$$

10.22060/EEJ.2026.25827.6010

where ΔP_{pv} and ΔP_{wtg} represent the output power variations of the PV and WTG units, respectively, while $\Delta\phi_{solar}$ and ΔP_{wind} denote the corresponding available power fluctuations due to changes in solar irradiance and wind speed. These sources are treated as non-dispatchable disturbances and do not participate directly in LFC.

Energy storage systems such as BESU and FESU provide fast frequency support and are modeled as first-order dynamic systems with proportional gain expressed by (11)-(12)

$$\Delta\dot{P}_{besu} = \frac{1}{T_{besu}}(-\Delta P_{besu} - \Delta f) \quad (11)$$

$$\Delta\dot{P}_{fesu} = \frac{1}{T_{fesu}}\left(-\Delta P_{fesu} - \Delta f\right) \quad (12)$$

where T_{besu} and T_{fesu} are the corresponding time constants. The negative sign with Δf ensures that the storage units inject power during frequency drops and absorb power during frequency rises, thereby stabilizing system frequency.

2.3 State-Space Representation

The overall microgrid system can be represented in state-space form by

$$\dot{x}(t) = Ax(t) + Bu(t) + Ed(t)$$

The state vector is given by

$$x(t) = \left[\Delta f \ \Delta P_m \ \Delta P_{deg} \ \Delta P_{f1} \ \Delta P_{f2} \ \Delta P_{fc} \ \Delta P_{p1} \ \Delta P_{p2} \ \Delta P_{pv} \ \Delta P_{wtg} \ \Delta P_{besu} \ \Delta P_{fesu}\right]^T$$

The control input vector is

$$u(t) = \left[\Delta U_{deg} \quad \Delta U_{fc}\right]^T$$

The disturbance vector is

$$d(t) = [\Delta P_d \quad \Delta\phi_{solar} \quad \Delta P_{wind}]^T$$

The system matrices are given by

10.22060/EEJ.2026.25827.6010

$$A=\begin{bmatrix}
-\frac{D}{2H} & 0 & \frac{1}{2H} & 0 & 0 & \frac{1}{2H} & 0 & 0 & \frac{1}{2H} & \frac{1}{2H} & \frac{1}{2H} & \frac{1}{2H}\\
-\frac{1}{RT_g} & -\frac{1}{T_g} & 0 & 0 & 0 & 0 & 0 & 0 & 0 & 0 & 0 & 0\\
0 & \frac{1}{T_t} & -\frac{1}{T_t} & 0 & 0 & 0 & 0 & 0 & 0 & 0 & 0 & 0\\
0 & 0 & 0 & -\frac{1}{T_{fc}} & 0 & 0 & 0 & 0 & 0 & 0 & 0 & 0\\
0 & 0 & 0 & \frac{1}{T_{in}} & -\frac{1}{T_{in}} & 0 & 0 & 0 & 0 & 0 & 0 & 0\\
0 & 0 & 0 & 0 & \frac{1}{T_{ic}} & -\frac{1}{T_{ic}} & 0 & 0 & 0 & 0 & 0 & 0\\
0 & 0 & 0 & 0 & 0 & 0 & -\frac{1}{T_{pv}} & 0 & 0 & 0 & 0 & 0\\
0 & 0 & 0 & 0 & 0 & 0 & \frac{1}{T_{in}} & -\frac{1}{T_{in}} & 0 & 0 & 0 & 0\\
0 & 0 & 0 & 0 & 0 & 0 & 0 & \frac{1}{T_{ic}} & -\frac{1}{T_{ic}} & 0 & 0 & 0\\
0 & 0 & 0 & 0 & 0 & 0 & 0 & 0 & 0 & -\frac{1}{T_{wtg}} & 0 & 0\\
-\frac{1}{T_{besu}} & 0 & 0 & 0 & 0 & 0 & 0 & 0 & 0 & 0 & -\frac{1}{T_{besu}} & 0\\
-\frac{1}{T_{fesu}} & 0 & 0 & 0 & 0 & 0 & 0 & 0 & 0 & 0 & 0 & -\frac{1}{T_{fesu}}
\end{bmatrix}$$

$$B=\begin{bmatrix}
0 & 0\\
\frac{1}{T_g} & 0\\
0 & 0\\
0 & \frac{1}{T_{fc}}\\
0 & 0\\
0 & 0\\
0 & 0\\
0 & 0\\
0 & 0\\
0 & 0\\
0 & 0\\
0 & 0
\end{bmatrix},\qquad E=\begin{bmatrix}
-\frac{1}{2H} & 0 & 0\\
0 & 0 & 0\\
0 & 0 & 0\\
0 & 0 & 0\\
0 & 0 & 0\\
0 & 0 & 0\\
0 & \frac{1}{T_{pv}} & 0\\
0 & 0 & 0\\
0 & 0 & 0\\
0 & 0 & \frac{1}{T_{wtg}}\\
0 & 0 & 0\\
0 & 0 & 0
\end{bmatrix}$$

The input and disturbance matrices are derived directly from the system dynamic equations (1)-(12), guaranteeing precise representation of control inputs and external disturbances to the state variables.

2.4 Discretized Model

For implementation of MPC, the continuous-time system is discretized using a zero-order hold (ZOH) method given by

$$x(k+1) = A_d x(k) + B_d u(k) + E_d d(k)$$

where A_d, B_d, and E_d are the discrete-time system matrices, and T_s denotes the sampling time. The matrices are obtained using standard ZOH discretization of the continuous-time model. This discrete-time representation is subsequently used for controller design and optimization in the proposed framework.

3 Laguerre-EDW Model Predictive Control

This section outlines the formulation of the Laguerre function-based MPC with EDW for LFC of the investigated microgrid. Employing Laguerre functions markedly reduces the computing demands inherent in conventional MPC by parameterizing the control input trajectory [2], [20].

3.1 Conventional MPC Formulation

For the discrete-time system described in Section 2, the predictive model is given by (13)

$$x(k+1) = A_d x(k) + B_d u(k) + E_d d(k) \tag{13}$$

The MPC objective is to minimize the following quadratic cost function

$$J = \sum_{i=1}^{N_p} x(k+i)^T Q x(k+i) + \sum_{i=0}^{N_c-1} u(k+i)^T R u(k+i) \tag{14}$$

In this context, N_p and N_c represent the prediction and control horizons, respectively, whereas Q and R signify the weighting matrices. This formulation provides optimal control performance; nevertheless, it necessitates addressing an optimization problem at each sampling instant, leading to significant computing complexity [21].

3.2 Laguerre Function-Based Control Parameterization

To reduce the computational burden, the control input sequence is parameterized using Laguerre functions. The control increment $\Delta u(k)$ is expressed by (15)

$$\Delta u(k+i) = \sum_{j=1}^{N_L} \eta_j(k) l_j(i) \tag{15}$$

where $l_j(i)$ represents the discrete Laguerre functions and $\eta_j(k)$ are the Laguerre coefficients to be optimized. The Laguerre functions are generated recursively given by (16) [20]

$$l_{j+1}(i) = a l_j(i) + \sqrt{1-a^2}\,\delta(i) \tag{16}$$

where a is the Laguerre pole parameter satisfying $0 \le a < 1$, and $\delta(i)$ is the unit impulse function.

10.22060/EEJ.2026.25827.6010

This parameterization decreases the quantity of decision variables from the control horizon N_c to the Laguerre order N_L, therefore substantially reducing computational complexity. The Laguerre pole parameter a dictates the dynamic properties of the Laguerre basis functions employed to parameterize the control trajectory. Lower values of a yield basis functions that decay more swiftly, leading to a more agile controller adept at promptly addressing frequency variations after load disturbances. Larger values of a produce smoother control trajectories with diminished control fluctuations, albeit at the expense of slower transient reactions. Consequently, selecting an acceptable value for a is crucial to attain an optimal equilibrium between disturbance rejection efficacy and control effort in microgrid LFC.

3.3 Exponential Data Weighting (EDW)

To improve transient performance and disturbance rejection capability, EDW is incorporated into the cost function. The updated cost function is expressed by (17)

$$J = \sum_{i=1}^{N_p} \alpha^i \, x(k+i)^T Q x(k+i) + \sum_{i=0}^{N_c-1} \alpha^i \, u(k+i)^T R u(k+i) \qquad (17)$$

where $\alpha \in (0,1]$ is the exponential weighting factor. The above approach prioritizes recent system states, hence improving the controller's responsiveness [22]. The exponential weighting factor α dictates the significance attributed to forecasted system states over the prediction horizon. Reduced values of α prioritize the near term, facilitating swifter corrective measures in response to abrupt disruptions. Conversely, values of α approaching unity distribute importance more evenly throughout the prediction horizon, resulting in more gradual control actions and enhanced long-term regulation. Thus, the choice of α directly affects the balance between transient responsiveness, frequency oscillation mitigation, and control effort.

3.4 Optimization Problem

The Laguerre-EDW MPC optimization problem can be formulated by (18)

$$\min_{\eta} J(\eta) \qquad (18)$$

subject to system dynamics and input constraints expressed by (19)

$$u_{min} \leq u(k) \leq u_{max} \qquad (19)$$

The optimal control sequence is derived by determining the Laguerre coefficients $\eta(k)$, with just the initial control input implemented at each sampling instant in accordance with the receding horizon concept. A formal proof of closed-loop stability is not provided in this study. The stability of the proposed control architecture is empirically validated by constrained system responses and well-damped frequency behavior seen under both step and random perturbations in load.

The efficacy of the Laguerre-EDW MPC depends on the sensible selection of a and α. Given that these factors collectively affect prediction accuracy, damping characteristics, control smoothness, and disturbance rejection capability, ascertaining appropriate values through manual

10.22060/EEJ.2026.25827.6010

tuning is challenging. This underpins the proposed ANN-assisted surrogate optimization paradigm outlined in the subsequent section.

4 Proposed ANN-Based Optimization Framework

Performance of the Laguerre-EDW MPC approach, on the other hand, depends significantly on how well the tuning parameters are chosen. To solve this problem, an optimization framework based on an ANN is suggested to efficiently determine the optimal parameters. This section introduces the proposed optimization framework utilizing an ANN for the tuning of Laguerre-EDW MPC parameters in LFC. The primary objective is to identify the best Laguerre pole parameter a and the exponential weighting factor α that reduce control costs while enhancing dynamic performance. Fig. 2 illustrates the overall control architecture of the proposed ANN-Laguerre-EDW MPC framework. The ANN provides optimal parameters to the controller, facilitating enhanced frequency control and reduced oscillations. The ANN is trained offline to understand the correlation between controller parameters and their respective control performance across a representative array of operating scenarios. During deployment, the trained ANN functions as a surrogate optimization model that swiftly predicts near-optimal Laguerre-EDW model predictive control parameters, therefore eliminating the necessity for repeated iterative optimization and substantially diminishing computational complexity.

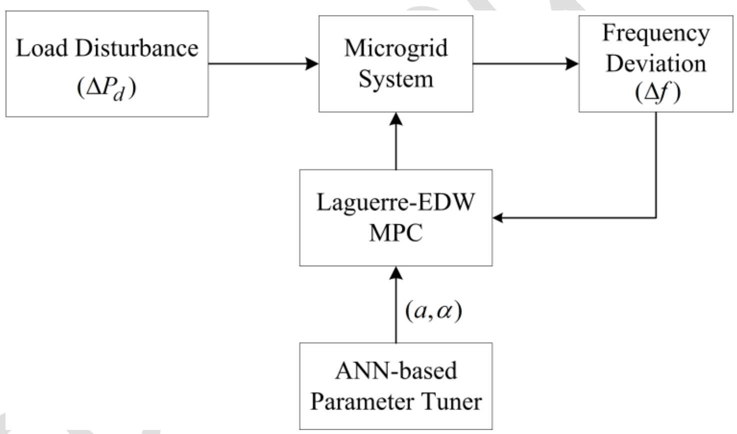

Figure 2: Overall control architecture of the proposed ANN-Laguerre-EDW MPC framework

4.1 Problem Formulation

The tuning problem can be formulated as an optimization problem represented by (20)

$$\min_{a,\alpha} J(a,\alpha) \tag{20}$$

where J denotes the MPC cost function as stated in Section 3. The parameters a and α substantially affect controller performance, and their optimal selection is complex.

10.22060/EEJ.2026.25827.6010

4.2 Training Data Generation

A training dataset is generated by uniformly sampling different combinations of (a, α) within their predefined bounds given by (21)

$$a \in [0,1), \qquad \alpha \in (0,1] \tag{21}$$

For each sampled parameter pair, the renewable-integrated microgrid is simulated under the specified operating scenario, and the corresponding MPC cost function J is evaluated. The generated input-output pairs form the training dataset

$$\mathcal{D} = \{(a_i, \alpha_i, J_i)\}_{i=1}^{N} \tag{22}$$

where N denotes the total number of training samples. Separate datasets are generated for different operational scenarios of the microgrid to accommodate their distinct disturbance characteristics and associated optimal controller parameters. The entire dataset is subsequently partitioned into training and testing sections with an 80:20 ratio. The training subset is utilized to develop the ANN surrogate model, whereas the testing subset is applied to assess its predictive performance and mitigate the risk of overfitting. The resulting supervised learning framework allows the ANN to estimate the nonlinear correlation between the controller parameters and the associated MPC performance index.

4.3 ANN Architecture

A feedforward multilayer perceptron (MLP) is utilized to mimic the nonlinear correlation between input parameters and the cost function. The architecture of the ANN is described as follows:

- Input layer: (a, α)
- Hidden layers: Two layers with nonlinear activation functions
- Output layer: Predicted cost $\hat{J}$

The ANN can be expressed as

$$\hat{J} = f_{\theta}(a, \alpha) \tag{23}$$

where θ denotes the network parameters (weights and biases). Neural networks are recognized for their universal approximation ability [23] and have been extensively applied in control optimization issues [9].

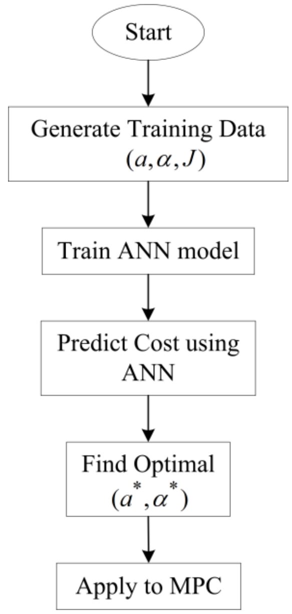

Figure 3: Flowchart of the proposed ANN-based optimization framework

4.4 Training Procedure

The ANN is trained using the generated dataset by minimizing the mean squared error (MSE) given by (24)

$$\mathcal{L} = \frac{1}{N}\sum_{i=1}^{N}(J_i - \hat{J}_i)^2 \tag{24}$$

where J_i and $\hat{J}_i$ represent the actual and expected cost values, respectively. Before training, the resulting dataset is randomly partitioned into training and testing groups in an 80:20 ratio. The training subset is utilized to refine the parameters of the ANN, whilst the testing subset assesses the predictive performance of the surrogate model and mitigates the risk of overfitting. The Adam optimizer is employed in gradient-based backpropagation to minimize the mean squared error loss function [24]. Separate ANN models are trained for different operating scenarios to accommodate their distinct disturbance characteristics and associated optimal controller parameters. Upon training completion, the ANN functions as a surrogate optimization model that swiftly evaluates controller performance for various combinations of (a, α), thus obviating the necessity for repetitive time-domain simulations throughout the parameter search process.

Upon concluding the training procedure, the trained ANN is utilized as a surrogate model to assess numerous candidate (a, α) combinations during the parameter search phase. The candidate evaluations conducted during this search are separate from the ANN training epochs.

4.5 ANN-Based Optimization

After training, the ANN is used to efficiently search for optimal parameters.

$$(a^*, \alpha^*) = \underset{a,\alpha}{\operatorname{argmin}} f_\theta(a, \alpha) \tag{25}$$

10.22060/EEJ.2026.25827.6010

This obviates the necessity for redundant system simulations, markedly diminishing computational complexity in contrast to metaheuristic methodologies. The efficacy of the ANN-based method is attributed to its capacity to approximate the nonlinear correlation between controller settings and system performance. In contrast to iterative optimization methods that necessitate multiple simulations, the trained ANN delivers nearly instantaneous predictions of the cost function. This significantly diminishes computing cost and facilitates rapid convergence to optimal parameter values, rendering the method computationally efficient for implementation compared with iterative optimization approaches. The overall procedure of the proposed ANN-based optimization framework is illustrated in Fig. 3. The ANN is trained to correlate controller parameters with performance, facilitating rapid prediction of optimal (α^*, α^*) without the need for redundant simulations.

The overall procedure of the proposed ANN-based optimization framework is summarized in Algorithm 1.

Algorithm 1 ANN-Based Optimization of Laguerre-EDW MPC

```
Generate dataset D = {(a_i, α_i, J_i)}
Initialize ANN parameters θ
Train ANN using MSE loss
while not converged do
    Update θ using gradient descent
end while
Use trained ANN to predict Ĵ (a, α)
Find optimal (a*, α*) = arg min Ĵ
Apply optimal parameters to MPC controller
```

4.6 Advantages and Limitations of the Proposed Approach

The proposed ANN-based approach offers the following advantages while exhibiting certain limitations as summarized in Table 2.

Table 2: Advantages and limitations of the proposed ANN-Laguerre-EDW MPC approach

Advantages	Limitations
Significant reduction in computational time due to elimination of iterative optimization	Requires extensive offline training data, which may increase initial computational effort
Ability to approximate complex nonlinear relationships between controller parameters and performance	Performance depends on quality and generalization capability of the trained ANN
Suitable for computationally efficient implementation due to fast parameter prediction after offline training	May require retraining if system dynamics change significantly (e.g., topology or operating conditions)
Improved tuning efficiency compared to	Lack of explicit stability guarantees due to data-

10.22060/EEJ.2026.25827.6010

Advantages	**Limitations**
metaheuristic methods such as PSO	driven tuning approach

Table 3: Controller and ANN parameters used in the study

Parameter	**Value**
MPC Parameters	
Prediction horizon (N_p)	20
Control horizon (N_c)	5
State weighting matrix (Q)	diag(300,1,1,10,10,10,10,10,400)
Control weighting (R)	0.2
Sampling time (T_s)	0.05 s
Laguerre Parameters	
Laguerre order (N_l)	5
Laguerre pole (a)	Optimized via ANN
Exponential weighting factor (α)	Optimized via ANN
ANN Architecture	
Input layer	2 neurons (a, α)
Hidden layers	2 layers (20 neurons each)
Activation function	Tanh
Output layer	1 neuron ($\hat{J}$)
ANN Training Parameters	
Training samples	500
Optimization method	Adam optimizer
Loss function	Mean Squared Error (MSE)
Epochs (max iterations)	500

5 Results and Discussion

This section provides a thorough assessment of the proposed ANN-Laguerre-EDW MPC controller in the contexts of diverse operating scenarios. The performance is evaluated against conventional PID, conventional MPC, Laguerre-EDW MPC, and PSO-Laguerre-EDW MPC controllers utilizing various performance metrics and statistical methods. The controller configuration and ANN training parameters used for the simulations are summarized in Table 3. Initial trials utilizing larger datasets (700 and 1000 samples) yielded only marginal enhancements in prediction accuracy while significantly escalating offline computational demands; hence, 500 samples was considered a suitable compromise.

10.22060/EEJ.2026.25827.6010

Figure 4: Performance comparison under 1% SLP: (a) frequency response, (b) zoomed frequency response, (c) cumulative cost, (d) control signals, (e) ISE, and (f) convergence of a

and α. Controllers: (1) Conventional PID, (2) Conventional MPC, (3) Laguerre-EDW MPC, (4) PSO-Laguerre-EDW MPC, (5) Proposed ANN-Laguerre-EDW MPC

5.1 Dynamic Performance under 1% Step Load Perturbation (SLP)

Fig. 4(a) depicts the frequency deviation response of the microgrid following a 1% SLP at t = 0 s. Simulation time is 50 s. The proposed ANN-Laguerre-EDW MPC demonstrates reduced oscillations with minimal overshoot relative to alternative control approaches. The conventional PID controller demonstrates greater oscillations and reduced damping owing to its fixed-parameter configuration. Despite enhancing the transient responsiveness, conventional MPC continues to experience mild oscillations attributable to inadequate parameter adjustment.

The Laguerre-EDW MPC mitigates oscillations by parameterizing the control trajectory; nevertheless, its efficacy is significantly influenced by the choice of a and α. The PSO-based control approach enhances tuning but results in more aggressive control actions, hence escalating control effort. The proposed ANN-based tuning yields a nearly optimal parameter configuration, leading to enhanced damping and expedited convergence.

The zoomed frequency response in Fig. 4(b) further substantiates that the proposed approach attains the minimal steady-state error and diminished oscillatory behavior, signifying enhanced disturbance rejection capabilities.

Fig. 4(c) illustrates that the proposed controller sustains a balanced cost profile in the cumulative cost comparison. Although PSO-Laguerre-EDW MPC initially attains a reduced cost through vigorous optimization, it ultimately incurs greater control effort and computing demands. The ANN-based approach, conversely, attains a more uniform cost trajectory, signifying effective control action without significant input fluctuations. The control signals (for FC and DEG) illustrated in Fig. 4(d) demonstrate that the suggested approach guarantees more stable actuator performance. This underscores the efficacy of the ANN in preventing sudden control fluctuations while preserving performance. The refined control signals evident in the proposed approach result from the evasion of drastic parameter adjustments commonly found in metaheuristic optimization techniques like PSO. The ANN-based tuning ensures reliable parameter selection, resulting in gradual and physically feasible control actions.

Table 4: Statistical performance comparison of various control approaches

Method	**Mean ISE**	**Std ISE**	**Mean Cost**	**Std Cost**
Conventional PID	1.23×10^{-5}	2.41×10^{-7}	0.000758	0.000087
Conventional MPC	0.96×10^{-5}	1.53×10^{-7}	0.005895	0.000157
Laguerre-EDW MPC	1.14×10^{-5}	2.57×10^{-7}	0.005315	0.000140
PSO-Laguerre-EDW MPC	2.55×10^{-5}	2.73×10^{-6}	0.003058	0.000099
ProposedANN-Laguerre-EDW MPC	0.81×10^{-5}	1.06×10^{-7}	0.005328	0.000169

Fig. 4(e) illustrates that the proposed ANN-based controller attains the minimal ISE compared to all other approaches, corroborating the statistical findings in Table 4. Table 4 displays the statistical comparison of controller performance regarding the mean and standard deviation of

10.22060/EEJ.2026.25827.6010

ISE and cost. The proposed ANN-Laguerre-EDW MPC demonstrates the lowest mean ISE and the smallest standard deviation, signifying both superior accuracy and consistency. Conversely, the PSO-Laguerre-EDW MPC demonstrates greater variability, indicating sensitivity to operational variables. While conventional MPC and Laguerre-EDW MPC demonstrate moderate efficacy, they do not attain the same degree of resilience as the proposed approach. These results confirm that the ANN-based tuning enhances performance while also guaranteeing dependable operation across diverse situations. This enhancement is attributed to the precise calibration of the a and α, which augments predictive accuracy and control responsiveness. Fig. 4(f) depicts the evolution of the optimal a and α throughout the ANN-based parameter search. The horizontal axis denotes the candidate parameter evaluations conducted with the trained ANN surrogate model, rather than the epochs of ANN training. The convergence behavior illustrates the rapid recognition of near-optimal controller parameters. As seen, a and α quickly converge to stable values (with a = 0.11 and α = 0.97), illustrating the efficacy of the surrogate model. In contrast to PSO, which necessitates iterative simulations, the ANN offers rapid parameter estimation, thereby markedly diminishing computer complexity.

The enhanced performance is attributed to the ANN's capacity to identify near-optimal tuning parameters that equilibrate prediction accuracy and control effort. The optimized a facilitates efficient control trajectory parameterization, while α improves response to recent system dynamics, leading to expedited damping and diminished oscillations.

5.2 Performance under Random Load Perturbation (RLP)

Figs. 5(a)-(f) show how optimally the suggested control approach works under RLP. Because the disturbance is random, all controllers display more oscillations than in the 1% SLP scenario. However, there are clear differences in robustness. Simulation time for this scenario is 180 s.

Fig. 5(a) demonstrates that the suggested ANN-Laguerre-EDW MPC approach possesses reduced frequency oscillations demonstrating better disturbance rejection. Conventional PID and MPC show bigger changes, while the PSO-based approach displays more changes since it uses

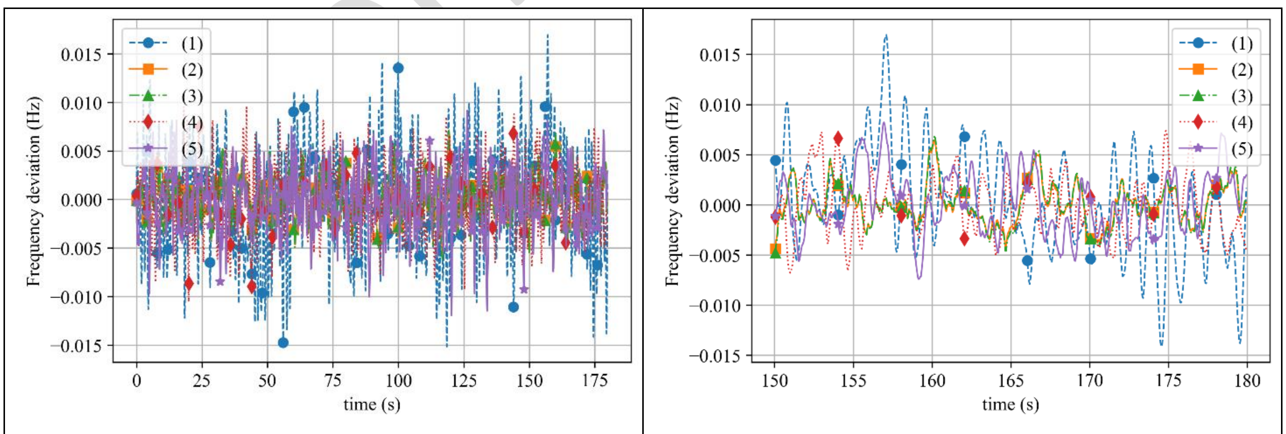

(a) (b)

10.22060/EEJ.2026.25827.6010

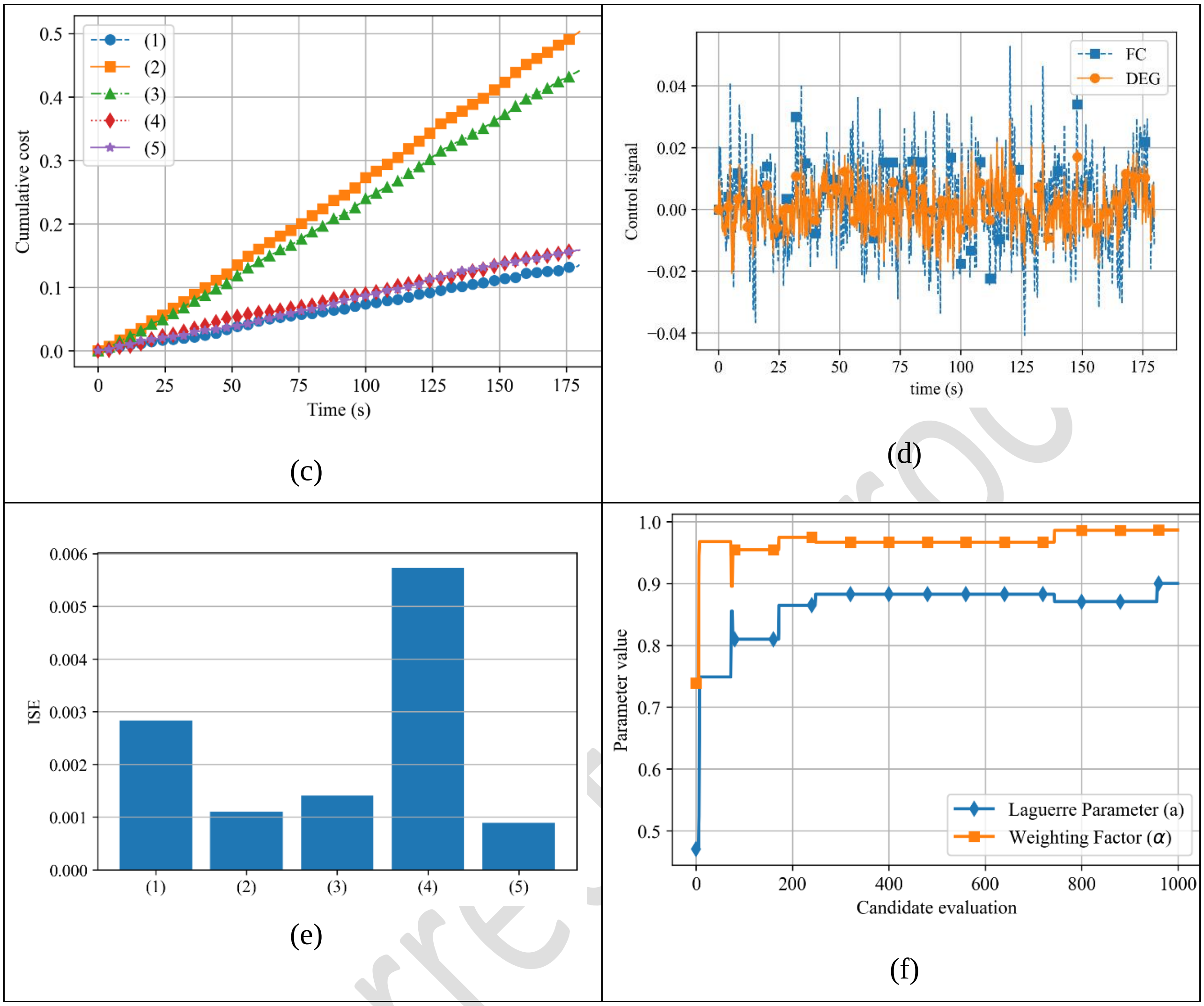

Figure 5: Performance comparison under RLP: (a) frequency response, (b) zoomed steady-state response, (c) cumulative cost, (d) control signals, (e) ISE, and (f) convergence of a and α. Controllers: (1) Conventional PID, (2) Conventional MPC, (3) Laguerre-EDW MPC, (4) PSO-Laguerre-EDW MPC, (5) Proposed ANN-Laguerre-EDW MPC

aggressive control action. The zoomed frequency response in Fig. 5(b) shows that the suggested approach keeps the frequency boundaries tighter with very little steady-state variation.

In Fig. 5(c), the total cost goes up for all controllers under RLP. However, the suggested approach keeps the cost trajectory balanced without requiring too much control effort. Fig. 5(d) displays that the control signals for FC and DEG are smoother, which means that the actuators are less stressed and the control is more consistent.

The proposed controller achieves the lowest ISE, as shown in Fig. 5(e). This validates that it can track better when subjected to random disturbances. Fig. 5(f) illustrates the convergence behavior of the ANN-assisted parameter search in response to RLP. The candidate evaluations demonstrate the continuous improvement of the optimal parameter pair forecasted by the trained

10.22060/EEJ.2026.25827.6010

ANN surrogate model (with α = 0.89 and α = 0.98). This shows that tuning with an ANN is more efficient than using iterative approaches.

In general, the suggested ANN-Laguerre-EDW MPC approach is more stable, better at controlling frequency, and more efficient at taking control actions corresponding to RLP scenario.

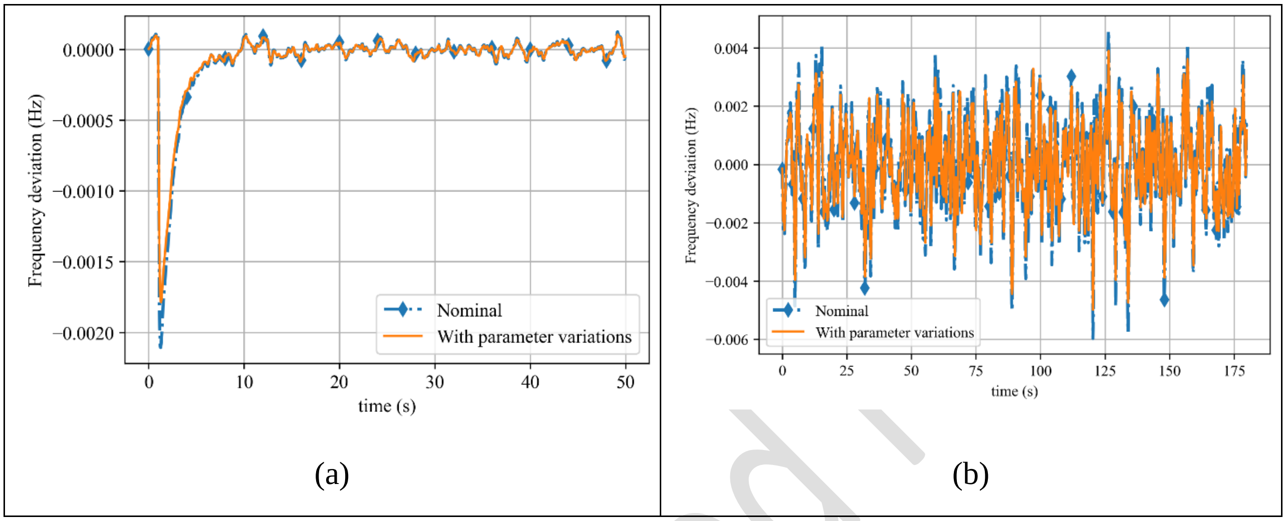

Figure 6: Sensitivity analysis showing frequency response for: (a) 1% SLP and (b) RLP

5.3 Sensitivity and Robustness Analysis

A sensitivity analysis is performed to assess the resilience of the proposed controller amidst parameter uncertainty. The parameters are concurrently adjusted as follows: $+25\%$ in H, -30% in D, -15% in R, -25% in T_g, $+35\%$ in T_t, -20% in T_{fc}, $+30\%$ in T_{besu}, and -30% in T_{fesu}. Fig. 6 displays the comparative frequency responses for both 1% SLP and RLP scenarios for nominal and varied parameter values.

The proposed ANN-Laguerre-EDW MPC exhibits stable and well-damped frequency responses even with considerable parameter fluctuations. Minor discrepancies in transient and steady-state behavior are noted under 1% SLP, but acceptable variations are sustained under RLP. This illustrates the efficacy of the suggested approach, owing to the ANN-based optimal parameter calibration and the improved sensitivity afforded by EDW. The constrained and adequately damped frequency responses in all circumstances further demonstrate the practical stability of the proposed control approach.

10.22060/EEJ.2026.25827.6010

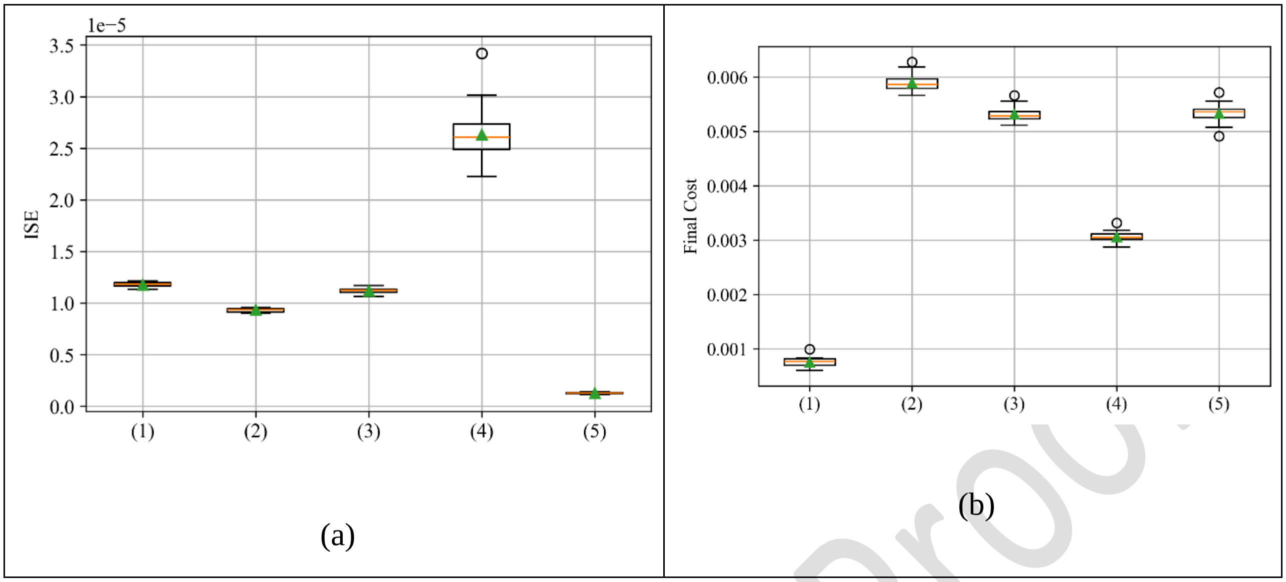

Figure 7: Boxplots for 20 independent trial runs for: (a) ISE and (b) cost

Table 5: ANOVA test results for ISE comparison

Parameter	**Value**
F-statistic	48.85
p-value	3.21×10^{-7}
Significance	Significant ($p < 0.05$)

Table 6: Pairwise t-test results for ISE comparison

Approach 1	**Approach 2**	**t-statistic**	**p-value**	**Significance**
Conventional PID	Conventional MPC	36.79	2.56×10^{-30}	Yes
Conventional PID	Laguerre-EDW MPC	7.55	5.04×10^{-9}	Yes
Conventional PID	PSO-Laguerre-EDW MPC	-24.65	4.67×10^{-16}	Yes
Conventional PID	Proposed ANN-Laguerre-EDW MPC	192.87	5.44×10^{-37}	Yes
Conventional MPC	Laguerre-EDW MPC	-25.47	1.02×10^{-23}	Yes
Conventional MPC	PSO-Laguerre-EDW MPC	-28.89	2.75×10^{-17}	Yes
Conventional MPC	Proposed ANN-Laguerre-EDW MPC	180.44	1.40×10^{-38}	Yes

10.22060/EEJ.2026.25827.6010

Approach 1	Approach 2	t-statistic	p-value	Significance
Laguerre-EDW MPC	PSO-Laguerre-EDW MPC	-25.64	1.96×10^{-16}	Yes
Laguerre-EDW MPC	Proposed ANN-Laguerre-EDW MPC	159.87	2.96×10^{-34}	Yes
PSO-Laguerre-EDW MPC	Proposed ANN-Laguerre-EDW MPC	42.66	2.37×10^{-20}	Yes

5.4 Statistical Validation

Boxplots for ISE values and cost given in Figs. 7(a)-(b) and Tables 5-6 confirm the superiority of the proposed approach. The Analysis of Variance (ANOVA) findings in Table 6 demonstrate a statistically significant difference across controllers, with a p-value substantially below 0.05. The paired t-test findings further validate that the proposed ANN-Laguerre-EDW controller markedly surpasses all the other approaches for ISE. It is to be noted that to perform statistical analysis 20 independent trial runs were made.

Table 7 presents a rating of controllers according to ISE and cost criteria. The proposed ANN-Laguerre-EDW MPC attains the highest ISE rank while sustaining a competitive cost rank, signifying an ideal equilibrium between performance and efficiency. Although the ANOVA and t-test findings indicate statistical significance ($p < 0.05$), it is also crucial to assess the practical significance of the enhancements. The decrease in ISE attained by the suggested ANN-based controller correlates with enhanced frequency regulation marked by reduced oscillation amplitude. In microgrid operation, this results in increased system stability, less actuator wear, and superior power quality provided to end users.

Table 7: Performance Ranking of Controllers

Method	ISE Rank	Cost Rank
Proposed ANN-Laguerre-EDW MPC	1	3
Conventional MPC	2	5
Laguerre-EDW MPC	3	4
Conventional PID	4	1
PSO-Laguerre-EDW MPC	5	2

Additionally, Table 8 compares the control effort and computational complexity for both 1% SLP and RLP scenarios. It has been noted that:

- Control effort escalates under RLP for all control approaches owing to recurrent disturbances.
- The PSO-Laguerre-EDW MPC approach demonstrates the greatest control effort and computing duration owing to iterative optimization.

10.22060/EEJ.2026.25827.6010

- The proposed ANN-Laguerre-EDW MPC controller demonstrates significantly reduced computing time relative to PSO-based MPC, while sustaining moderate control effort.
- The Laguerre-EDW structure significantly decreases computational requirements relative to conventional MPC.

The statistical analysis is conducted exclusively for the 1% SLP scenario due to its deterministic and repeatable nature, which enables the establishment of consistent comparisons across a multitude of trial runs. However, the RLP scenario is stochastic, which means that the disturbances are not consistent and renders it challenging to employ conventional statistical tests. Therefore, the RLP's efficiency is evaluated through time-domain simulations and error metrics, which demonstrate that the proposed controller is sufficiently robust.

Overall, the proposed ANN-Laguerre-EDW MPC approach achieves an optimal balance among dynamic performance, control effort, and computational efficiency, rendering it appropriate for computationally constrained microgrid control applications.

Table 8: Comparison of Control Effort and Computational Complexity

Controller	**Control Effort**	**Avg. Computation Time (s)**	**Complexity Level**
	SLP		
Conventional PID	5.16×10^{-3}	0.062	Low
Conventional MPC	8.67×10^{-3}	0.739	High
Laguerre-EDW MPC	6.81×10^{-3}	0.493	Medium
PSO-Laguerre-EDW MPC	9.88×10^{-3}	5.411	Very High
Proposed ANN-Laguerre-EDW MPC	6.19×10^{-3}	0.308	Medium-Low
	RLP		
Conventional PID	7.74×10^{-3}	0.093	Low
Conventional MPC	14.73×10^{-3}	1.219	High
Laguerre-EDW MPC	11.58×10^{-3}	0.789	Medium
PSO-Laguerre-EDW MPC	18.29×10^{-3}	8.928	Very High
Proposed ANN-Laguerre-EDW MPC	9.91×10^{-3}	0.473	Medium-Low

5.5 Practical Implementation Considerations

The proposed ANN-based Laguerre-EDW MPC framework provides a computationally efficient substitute for iterative optimization by utilizing an offline-trained ANN as a surrogate optimization model. Upon training, the ANN rapidly forecasts the ideal Laguerre pole and exponential weighting factor without necessitating iterative optimization during controller execution, thus markedly alleviating the computing load in comparison to PSO-based tuning. Table 7 indicates that the proposed approach exhibits enhanced execution efficiency while preserving adequate control performance. The ANN is trained offline and does not adjust its

10.22060/EEJ.2026.25827.6010

parameters based on real-time system metrics during operation. Consequently, the suggested framework facilitates rapid parameter estimation but lacks the capability for adaptive online tuning in response to varying operating conditions.

Future work will focus on developing adaptive ANN-assisted MPC frameworks that employ real-time system feedback for continuous parameter adjustment and improved resilience under fluctuating microgrid conditions.

6 Conclusion

This paper proposes an ANN-based optimal tuning framework for Laguerre-EDW MPC in LFC in renewable-integrated microgrids, utilizing the ANN as a surrogate model to eliminate iterative optimization and facilitate swift parameter tuning. The simulation outcomes under both 1% SLP and RLP scenarios indicate that the proposed approach substantially improves dynamic performance, resulting in reduced frequency oscillations and negligible steady-state error in comparison to conventional PID, MPC, Laguerre-EDW MPC, and PSO-Laguerre-EDW MPC approaches. The controller attains a reduction of up to 68% in ISE, accompanied by smoother control signals, signifying greater system stability, diminished actuator stress, and improved power quality. The proposed framework significantly reduces processing demands, attaining up to a 95% decrease in calculation time compared to PSO-based tuning, thereby rendering it appropriate for real-time applications. Sensitivity analysis verifies strong performance amid substantial parameter fluctuations, while statistical validation through numerous trial runs demonstrates the approach's consistency and stability. The proposed ANN-based approach substantially diminishes computational demands via offline surrogate optimization; nonetheless, the controller parameters remain fixed during online operation. Future research will explore online adaptive and reinforcement learning approaches for parameter adjustment under varying operating conditions.

The proposed approach can be adapted for real-time execution utilizing hardware-in-the-loop (HIL) platforms and implemented in multi-area microgrids, accounting for communication latencies, cyber-physical limitations, and increased renewable integration.

Availability of data and material:
The data supporting the findings of this study are generated through simulations and are available from the corresponding author upon reasonable request. No external datasets were used.

Competing interests:
The author(s) declare that they have no competing interests.

Funding:
This research received no specific grant from any funding agency in the public, commercial, or not-for-profit sectors.

Authors' contributions:
The author conceived the study, developed the methodology, performed simulations, analyzed the results, and wrote the manuscript. The author has read and approved the final manuscript.

Acknowledgements:
The author would like to thank the Department of Electrical Engineering, Parala Maharaja Engineering College, for providing the necessary computational facilities and research support.

References

[1] I. Khan et al., "New trends and future directions in load frequency control: A comprehensive review," Alexandria Eng. J., 2023.

[2] P. Wang et al., "A MPC-based load frequency control considering wind power intelligent forecasting," Renew. Energy, 2025.

[3] B. Khokhar, K. S. Parmar, T. Thakur, and D. Kothari, Load Frequency Control of Microgrids. CRC Press, 2024.

[4] E. Oliveira et al., "Optimal transient droop compensator and PID tuning for load frequency control," Int. J. Electr. Power Energy Syst., vol. 73, pp. 888–898, 2015.

[5] Z. Wu et al., "Optimized cascaded PI controller for load frequency regulation," Energy Rep., vol. 8, pp. 450–461, 2022.

[6] K. Kang et al., "Distributed model predictive load frequency control for virtual power plants," Energies, vol. 18, no. 6, p. 1380, 2025.

[7] A. Rehiara, "Laguerre function-based model predictive control for load frequency control," TELKOMNIKA, vol. 16, no. 4, pp. 1540–1548, 2018.

[8] M. Irfan et al., "Optimizing load frequency control in microgrid with vehicle-to-grid integration," Appl. Energy, vol. 355, p. 122250, 2024.

[9] I. Mohamed et al., "Neural network-based model predictive control of power converters," IEEE Trans. Ind. Electron., vol. 67, no. 8, pp. 6500–6510, 2019.

[10] M. A. Khan et al., "Real-time adaptive load frequency control in hybrid PV-fuel cell microgrids," Int. J. Electr. Power Energy Syst., vol. 156, p. 109700, 2025.

[11] M. S. Souderjani and M. H. Golshan, "Narx neural network-based black-box equivalence model of external microgrids in a multi-microgrid including dfig and bess," Electr. Power Syst. Res., vol. 235, p. 112720, 2026.

[12] A. Abdulaziz et al., "AI-enhanced load frequency control in multi-area power systems," Results Eng., vol. 26, p. 104230, 2025.

[13] S. Sengar and X. Liu, "An efficient load forecasting in predictive control strategy using hybrid neural network," J. Circuits Syst. Comput., vol. 29, no. 01, p. 2050010, 2020.

10.22060/EEJ.2026.25827.6010

[14] S. Saadatmand, P. Shamsi, and M. Ferdowsi, "Power and frequency regulation of synchronverters using a model free neural network-based predictive controller," IEEE Trans. Ind. Electron., vol. 68, no. 5, pp. 3662–3671, 2021.

[15] H. H. Ali et al., "A novel sooty terns algorithm for deregulated MPC-LFC installed in multi-interconnected system with renewable energy plants," Energies, vol. 14, no. 17, p. 5393, 2021.

[16] S. D. Al-Majidi et al., "Design of a load frequency controller based on an optimal neural network," Energies, vol. 15, no. 17, p. 6223, 2022.

[17] M. Dashtdar, A. Flah, S. M. S. Hosseinimoghadam, and A. El-Fergany, "Frequency control of the islanded microgrid including energy storage using soft computing," Sci. Rep., vol. 12, no. 1, p. 20409, 2022.

[18] E. Yaghoubi et al., "A systematic review and meta-analysis of model predictive control in microgrids: Moving beyond traditional methods," Processes, vol. 13, no. 7, p. 2197, 2025.

[19] Z. G. Ma, M. Værbak, L. Cong, J. D. Billanes, and B. N. Jørgensen, "Enhancing island energy resilience: Optimized networked microgrids for renewable integration and disaster preparedness," Electronics, vol. 14, no. 11, p. 2186, 2025.

[20] A.-T. Tran, V. Van Huynh et al., "Load frequency control design for complex power systems implementing integral single-phase sliding mode control," Eng. Technol. Appl. Sci. Res., vol. 15, no. 1, pp. 19802–19808, 2025.

[21] M. A. Shehu et al., "Control and energy management of standalone microgrids in remote areas: A review of recent advances, challenges, and opportunities for future research," Eng. Sci. Technol. Int. J., vol. 75, p. 102288, 2026.

[22] H. Bevrani, F. Habibi, P. Babahajyani, M. Watanabe, and Y. Mitani, "Intelligent frequency control in an AC microgrid: Online PSO-based fuzzy tuning approach," IEEE Trans. Smart Grid, vol. 3, no. 4, pp. 1935–1944, 2012.

[23] Y. A.-R. I. Mohamed and E. F. El-Saadany, "Microgrid modeling and simulation," IEEE Trans. Power Syst., vol. 23, no. 3, pp. 964–972, 2008.

[24] N. Hatziargyriou, H. Asano, R. Iravani, and C. Marnay, "Microgrids: An overview of ongoing research, development, and demonstration projects," IEEE Power Energy Mag., vol. 5, no. 4, pp. 78–94, 2007.

[25] R. H. Lasseter, "Microgrids," in IEEE Power Engineering Society Winter Meeting, vol. 1, 2002, pp. 305–308.

[26] B. Khokhar and K. Singh Parmar, "Frequency regulation in a microgrid integrating redox flow battery by utilizing an optimal predictive control approach," Electr. Eng., vol. 106, no. 4, pp. 4257–4275, 2024.

[27] B. Khokhar and K. P. S. Parmar, "Impact analysis of capacitive energy storage integration on load frequency control performance of microgrids employing a new dual-stage controller," ISA Trans., vol. 162, pp. 162–178, 2025.

10.22060/EEJ.2026.25827.6010

[28] H. Bevrani, Robust Power System Frequency Control. Berlin, Germany: Springer, 2009.

[29] L. Wang, Model Predictive Control System Design and Implementation Using MATLAB. London, U.K.: Springer, 2009.

[30] E. F. Camacho and C. Bordons, Model Predictive Control, 2nd ed. London, U.K.: Springer, 2013.

[31] J. A. Rossiter, Model-Based Predictive Control: A Practical Approach. Boca Raton, FL, USA: CRC Press, 2003.

[32] K. Hornik, M. Stinchcombe, and H. White, "Multilayer feedforward networks are universal approximators," Neural Netw., vol. 2, no. 5, pp. 359–366, 1989.

[33] D. P. Kingma and J. Ba, "Adam: A method for stochastic optimization," in Int. Conf. Learn. Represent. (ICLR), 2015.